Polymer 51 (2010) 291–299

Contents lists available at ScienceDirect

Polymer

journal homepage: www.elsevier.com/locate/polymer

# Molecular dynamics and dissipative particle dynamics simulations for the miscibility of poly(ethylene oxide)/poly(vinyl chloride) blends

Zhonglin Luo, Jianwen Jiang*

*National University of Singapore, Department of Chemical and Biomolecular Engineering, 117576 Singapore*

ARTICLE INFO

*Article history:*
Received 16 September 2009
Received in revised form
11 November 2009
Accepted 12 November 2009
Available online 18 November 2009

*Keywords:*
PEO
PVC
Miscibility

ABSTRACT

The miscibility of poly(ethylene oxide) (PEO)/poly(vinyl chloride) (PVC) blends are investigated by atomistic molecular dynamics and mesoscale dissipative dynamics simulations. The specific volumes of three PEO/PVC blends (with weight ratio at 70/30, 50/50 and 30/70) as well as pure PEO and PVC are examined as a function of temperature. The glass transition temperatures are estimated to be 251, 268, 280, 313 and 350 K for pure PEO, PEO/PVC 70/30, 50/50, 30/70 and pure PVC. Among different energy contributions, the torsion and van der Waals energies exhibit pronounced kinks versus temperature. The Flory–Huggins parameters determined from the cohesive energy densities and the radial distribution functions of the inter-molecular atoms suggest that PEO/PVC 70/30 and 30/70 blends are more miscible than 50/50 blend. This is further supported by the morphologies of PEO/PVC blends, in which the 50/50 blend exhibits segregated domains implying a weak phase separation. Hydrogen bonds are found to form between O atoms of PEO and H atoms of PVC, with a larger degree in PEO/PVC 70/30 and 30/70 blends than in 50/50 blend. The addition of PVC into PEO suppresses the mobility of PEO chains, which is consistent with the experiment observation of decreased crystallization rate as well as crystallization temperature of PEO.



## 1. Introduction

Poly(ethylene oxide) (PEO) is one of the most commercially used polyethers and also known as poly(ethylene glycol) (PEG). While PEO and PEG contain the same repeat unit [$CH_2$–O–$CH_2$], oligomers with molecular weight below 20,000 g/mol are historically called PEG or otherwise called PEO. In recent decades, there has been considerable interest in using PEO or PEG as membrane material for $CO_2$ capture because of the strong affinity of PEO segments for $CO_2$ [1,2]. However, pure PEO tends to crystallize and fails to form homogenous and defect-free membranes [1]. In additional, it cannot be used at high temperatures and pressures due to weak mechanical property [3,4]. As a consequence, modified PEO membranes by cross-linking, copolymerization or blending become more attractive, such as photo-polymerized PEO network from mono- and dimethacrylate PEG oligomers [5,6], PEO/polyimide copolymers [7,8], PEO blends with cellulose nitrate [9] or cellulose acetate [10,11].

Poly(vinyl chloride) (PVC) has a high mechanical strength and wear-resistance [12]. It is a common plastic and widely used in construction sector, food package and toy factory. Compared to polyimides and celluloses, PVC is relatively cheaper and ideal for the formation of PEO/PVC blends. It has been demonstrated that the addition of PVC into PEO improves the mechanical property of PEO membranes [13] and suppresses the crystallization of PEO [14–16]. PEO/PVC membrane is thus a potential commercial product for gas separation. The performance of PVC/PEG4000 dense membranes with PEG weight contents (wt%) of 20% and 30% was found to be above the Robeson's selectivity/permeability upper-bound for $CO_2$/$N_2$ and $CO_2$/$CH_4$ mixtures [17].

Intuitively, PEO/PVC blends are miscible based on the factor that the O atoms in EO units can form hydrogen bonds (H-bonds) with the H atoms in CHCl group of PVC [15,18]. Furthermore, the electron-rich O atoms in PEO may act as donors and have attractive interactions with the electron-deficient Cl atoms in PVC [14,19,20]. A number of experiments were conducted in the past to investigate the compatibility of PEO and PVC with various compositions and two conclusions were usually reported. By dynamic mechanical analysis, differential scanning calorimetry and optical microscopy, Margaritis and Kalfoglou [21] observed that PEO and PVC were miscible for PVC-rich blends. Marco et al. [15] had a similar conclusion by $^{13}C$ NMR study that PEO/PVC blend was thermodynamically stable at PVC wt% > 40%. In contrast, Castro et al. [14] pointed out that PEO/PVC blends were miscible at PVC wt% < 60 wt% by determining the crystallization rate and crystallization temperatures of pure PEO and

* Corresponding author.
*E-mail address:* chejj@nus.edu.sg (J. Jiang).

0032-3861/$ – see front matter © 2009 Elsevier Ltd. All rights reserved.
doi:10.1016/j.polymer.2009.11.024

PEO/PVC blends. By inverse gas chromatography (IGC) to detect the interaction parameters in various solvents at 373 K, Etxeberria et al. [18] found that the blends were more miscible at high PVC content (80 wt% PVC) or PEO content (80 wt% PEO), while the two polymers were less compatible at PEO/PVC composition of 50/50.

Despite the above-mentioned experimental studies, the miscibility of PEO/PVC blends remains elusive. With the ever-growing computational power and resource, molecular simulations have played increasingly important role in materials modeling and subsequent technology development, as they can reveal the microscopic pictures of underlying mechanisms that are otherwise experimentally inaccessible or difficult to obtain. In this work, we investigate the thermodynamic, structural and dynamic properties of PEO/PVC blends as well as pure PEO and PVC using molecular simulations. Following this Section, the simulation models and protocols are described in Section 2 with fully atomistic scale molecular dynamics (MD) and mesoscale dissipative particle dynamics (DPD) simulations. In Section 3, the glass transition, Flory–Huggins parameter, radial distribution functions, hydrogen bonds, and dynamics of polymer chains are presented and discussed in detail for polymer blends and pure polymers. In addition, the morphologies of blends are also examined.

## 2. Simulation models and protocols

### 2.1. Molecular dynamics

MD simulations were performed to study the atomistic models of PEO/PVC blends using Material Studio [22]. Polymer chains were first built from EO and VC repeat units, and then cubic simulation boxes were constructed with the Amorphous Cell module based on the packing technique of Theodorou and Suter [23,24] and Meirovitch scanning method [25]. Table 1 lists the PEO/PVC blends of different weight compositions (including pure polymers) examined in the MD simulations. The number of units, chains and atoms, initial densities, and box lengths are also summarized in Table 1. For each system, 100 configurations were constructed and COMPASS [26–28] force field was used for the MD simulations. The total potential energy ($E_{pot}$) was expressed as

$$\begin{aligned} E_{pot} &= E_{bond} + E_{nonbond} + E_{cross} \\ &= E_b + E_\theta + E_\phi + E_{vdW} + E_{Coulombic} + E_{cross} \end{aligned} \quad (1)$$

where $E_b$ is the bond stretching energy, $E_\theta$ is the angle bending energy, $E_\phi$ is the dihedral torsion energy; the sum of these three items is the bonded energy ($E_{bond}$). $E_{vdW}$ is the van der Waals energy, $E_{coulomb}$ is the Coulombic energy; and the sum is the nonbonded energy ($E_{nonbond}$). $E_{cross}$ is the energy of cross terms between any two of the bonded items, such as the bond-angle cross term and the bond-bond cross term.

**Table 1**
PEO/PVC blends of different compositions considered in MD Simulations.

| PEO/PVC compositions | Number of EO units | Number of VC units | Number of chains | Initial density (g/cm$^3$) | Number of atoms | Box length (Å) |
|---|---|---|---|---|---|---|
| 100/0 | 90 | – | 2 PEO | 1.125[a] | 1264 | 22.71 |
| 70/30 | 90 | 54 | 2 PEO/ 1 PVC | 1.21 | 1590 | 24.94 |
| 50/50 | 142 | 100 | 1 PEO/ 1 PVC | 1.26 | 1598 | 25.42 |
| 30/70 | 90 | 150 | 1 PEO/ 1 PVC | 1.31 | 1534 | 25.64 |
| 0/100 | – | 100 | 2 PVC | 1.39[b] | 1204 | 24.63 |

[a] From the product catalogue of Sigma–Aldrich Inc. The density of PEO is 1.07 ~ 1.27 g/cm$^3$.
[b] From Ref. [12], the density of PVC is 1.37 ~ 1.43 g/cm$^3$. Other densities were calculated by the weight average of PEO and PVC.

To eliminate the unfavorable contacts, the 100 initial configurations were subjected to 50,000 steps of energy minimization by the Forcite module with the energy convergence threshold of $1 \times 10^{-4}$ kcal mol$^{-1}$ and the force convergence of 0.005 kcal mol$^{-1}$ Å$^{-1}$. The Ewald summation was adopted for the Coulombic interactions with an accuracy of 0.01 kcal mol$^{-1}$, and the atom-based summation was applied for the van der Waals interactions with a cutoff distance of 9.5 Å, a spline width of 1 Å, and a buffer width of 0.5 Å. For pure PEO and PVC systems, the first 6–7 configurations with the lowest energy were chosen for subsequent MD simulations. For PEO/PVC blends, the configurations with the lowest energy were examined to ensure sufficient contacts of the two polymers by calculating the inter-molecular radial distribution functions $g(r)$ of the carbon atoms between PEO and PVC. If the $g(r)$ was lower than that of pure PEO and PVC which indicated the two polymers were not mixed well, the configuration was discarded and another with a relative higher energy was further considered.

For each system, all the chosen configurations were subject to a 10-circle thermal annealing from 300 to 1000 K and then back to 300 K with 50 K intervals. At each temperature, 10 ps MD simulation was performed at constant pressure (1 bar) with a time step of 1 fs. The temperature and pressure were maintained by the Berendsen method [29]. At a very high temperature, the annealing might terminate if the energy deviation between two successive steps was larger than a specified value 5000 kcal mol$^{-1}$, especially in PEO-containing systems. At this situation, the last configuration was further subject to a 50,000-step energy minimization and followed by annealing. After the 10-cirle annealing, equilibrium MD simulation was performed at 500 K and 1 bar for 1 ns. Then the system was cooled down stepwise to 120–200 K at 20 K intervals. At each temperature, 100 ps equilibrium was carried out at constant volume and then 250 ps simulation at 1 bar. Trajectories were saved every 5 ps and the final 50 ps configurations were used for analysis.

### 2.2. Dissipative particle dynamics

DPD is a mesoscale method for the simulations of coarse-grained systems over long length and time scales. In DPD several atoms or repeat units are grouped together and presented by a single bead, thus the algorithm increases simulation scale by several orders of magnitude compared to atomistic simulation. A polymer chain in DPD can be considered to consist of $n_{DPD}$ beads

$$n_{DPD} = \frac{M_p}{M_m C_n} = \frac{n}{C_n} \quad (2)$$

where $M_p$ is the molar mass of the polymer, $M_m$ is the molar mass of repeat unit, $n$ is the number of repeat units, and $C_n$ is the characteristic ratio of the polymer and used to determine how many repeated units should be grouped into one bead. Based on the connectivity indices for polymer chain as proposed by Bicerano [30], $C_n$ can be evaluated using the Synthia module in Materials Studio. For PEO and PVC, $C_n$ were estimated to be 4.98 and 6.86, respectively. The chain lengths of the three blends (PEO/PVC 70/30, 50/50 and 30/70 blends) considered in our study are listed in Table 2.

The motion of beads in DPD is governed by a force function as [31]

$$f_i = \sum_{j \neq i} \left( F_{ij}^C + F_{ij}^D + F_{ij}^R \right) + f_i^S + f_i^A \quad (3)$$

where $F_{ij}^C$ is the conservative repulsive force representing excluded volume, $F_{ij}^D$ is dissipative force representing the viscous drag between moving beads, and $F_{ij}^R$ is the random force representing

**Table 2**
Parameters in DPD simulations at $k_BT = 1.0$ corresponding to an atomic temperature $T = 300$ K.

| PEO/PVC compositions | Chain length of PEO | Chain length of PVC | $\chi_{AB}$ | $a_{AB}$ |
|---|---|---|---|---|
| 70/30 | 23 | 10 | −0.12 | 24.580 |
| 50/50 | 20 | 10 | 0.17 | 25.595 |
| 30/70 | 10 | 12 | −0.17 | 24.405 |

stochastic impulse. Both $F_{ij}^D$ and $F_{ij}^R$ act together as a thermostat for the beads. The remaining terms are bonded interactions: springs (S) controlling the bond stretching and angles (A) representing angle bending. All forces are short-ranged and effective within a cutoff radius $r_c$, which is usually set as a unit length. Similarly, the bead mass $m$ is assumed as a unit mass and the thermal energy $k_BT$ as a unit energy. All other properties are scaled accordingly with respect to $r_c$, $m$, and $k_BT$.

By studying a pure liquid system in which each molecule was presented as a DPD bead, Groot and Warren [32] first developed a relationship for the conservative force parameter $a$, density $\rho$, and pressure $p$ as $p = \rho k_BT + \alpha a \rho^2$ at $\rho > 2$, where the coefficient $\alpha = 0.101$. This implies that the compressibility could be given by $\kappa^{-1} = 1 + 2\alpha a\rho/k_BT$. Based on the compressibility for water $\kappa^{-1} = 16$ at 300 K, they proposed $a = 75k_BT/\rho$. In principle, the density chosen in DPD simulation is a free parameter, but the system with a larger $\rho$ requires a longer computational time. Groot and Warren [32] suggested that $\rho = 3$ and hence $a = 25k_BT$ are reasonable parameters for liquids. Moreover, they studied binary mixtures A and B presenting monomers and polymers. By assuming $a_{AA} = a_{BB}$ for AA and BB contacts, they found a linear relationship between AB contacts $a_{AB}$ and the Flory–Huggins interaction parameter $\chi$ as $a_{AB} = a_{AA} + 3.50\chi$. The $\chi$ value could be measured experimentally or calculated from atomistic simulations. In this work, the DPD simulations for the three PEO/PVC blends were conducted using Materials Studio. For each blend, the total number of beads was $2.4 \times 10^4$ in a simulation cell $20 \times 20 \times 20$. The production run was $2 \times 10^5$ steps with a time step 0.05. The thermal energy $k_BT = 1$ was used to maintain the default values of dissipation parameter 4.5 and spring constant 4.0 as well as $a_{AA}$ and $a_{BB}$.

## 3. Results and discussion

In the literature, short oligomers with ten or slightly more repeated units were usually used to simulate the miscibility of polymers [33–36]. Such short chains might lead to end effects and cannot represent the real systems accurately. On the other hand, one also wants to avoid using very long chains because of demanding simulation time. To determine the appropriate chain lengths for PEO and PVC in our study, the density and solubility parameter were examined as a function of chain length. As shown in Fig. 1, the density of PEO or PVC increases with increasing chain length; in contrast, the solubility parameter decreases. For PEO, when the number of monomers reaches 40, the density and solubility parameter are almost constant; thus 40 repeat units are sufficient to present a PEO chain. For PVC, the solubility does not change significantly for 50-mers and longer chains. Therefore, PVC with length of 50 is reasonable to present a polymer. In our study, the chain lengths for different systems are listed in Table 1.

### 3.1. Glass transition

At glass transition temperature $T_g$, there is a characteristic change in the motion of polymer chains. The occurrence of $T_g$ can be used as a rule of thumb to determine the compatibility of blend.

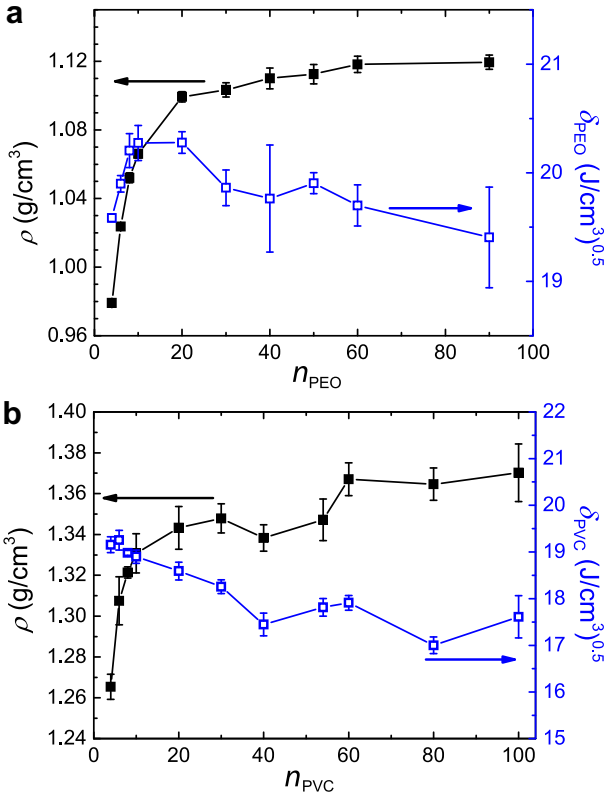


**Fig. 1.** Density and solubility parameter as a function of chain length for (a) PEO and (b) PVC.

If a binary blend is miscible, only a single $T_g$ appears [37]. Otherwise, two $T_g$'s could be detected and each $T_g$ indicates the frozen temperature of one component [38]. Fig. 2 shows the specific volume (reciprocal of density) as a function of temperature for pure PEO and PVC as well as their blends. A distinct kink in each curve indicates the occurrence of glass transition. For each system, only one $T_g$ is observed. Thus it could be preliminarily concluded that PEO/PVC blends are miscible at the three compositions 70/30, 50/50 and 30/70 considered. The estimated $T_g$'s are 251, 268, 280, 313, and 350 K for pure PEO, PEO/PVC 70/30, 50/50, 30/70 and pure

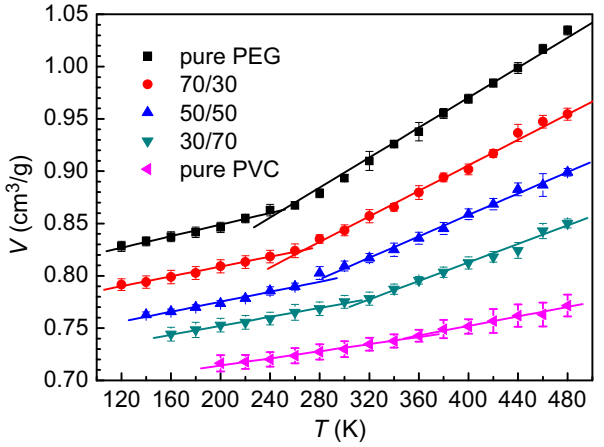


**Fig. 2.** Specific volume as a function of temperature. The glass transition temperature $T_g$ is estimated at 251, 268, 280, 313 and 350 K for pure PEO (■), PEO/PVC 70/30 (●), 50/50 (▲), 30/70 (▼), and pure PVC (◄).

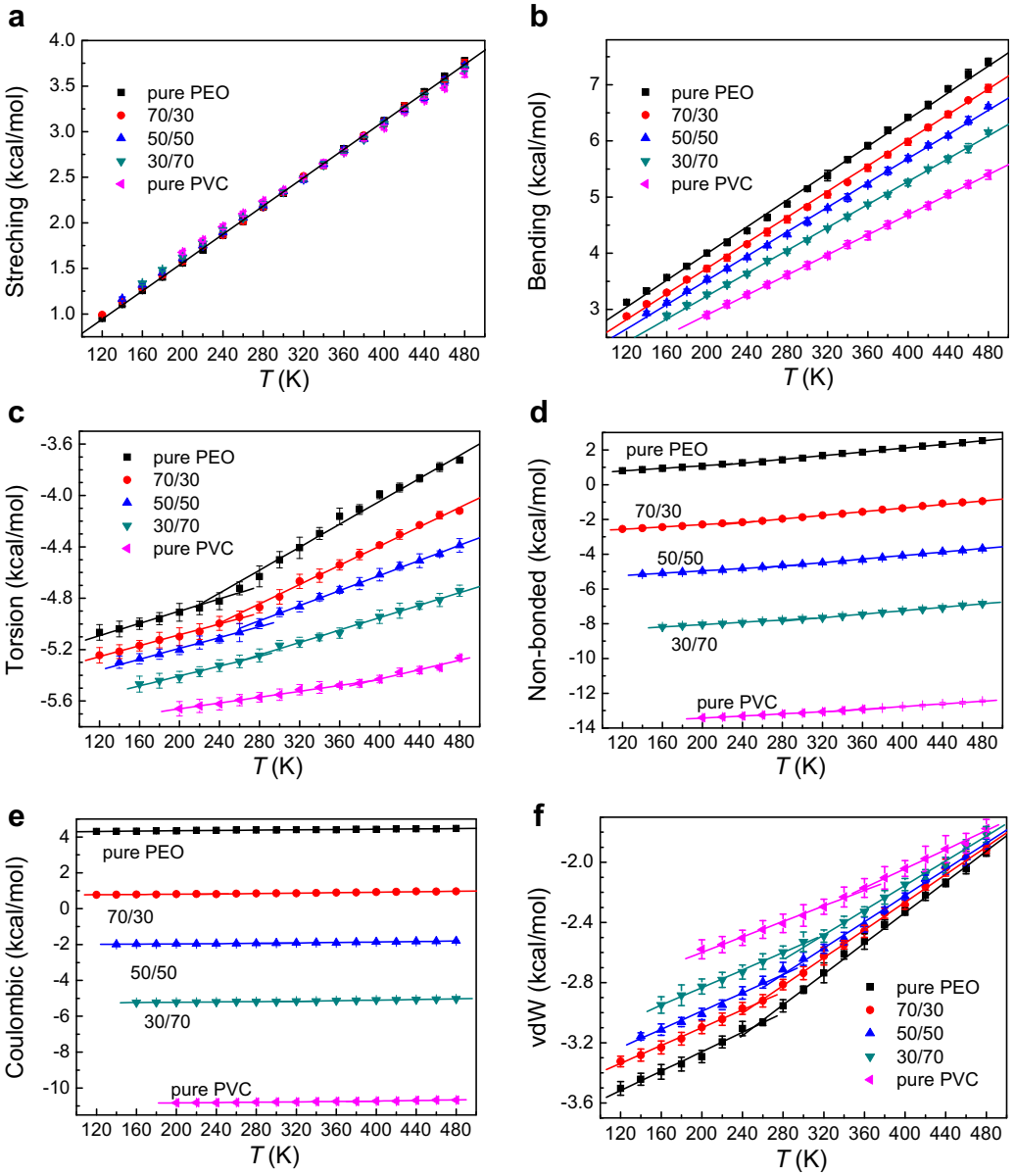


**Fig. 3.** Energy per repeat unit as a function of temperature. The legends are the same as in Fig. 2.

PVC, respectively. The experimental $T_g$ for pure PEO with a high molecular weight is around 158 ~ 233 K [39]. Faucher et al. found that $T_g$ of PEO decreases from 256 to 200 K upon its molecular weight changing from 6000 to 200,000 g/mol [40]. $T_g$ of pure PVC is about 360 K experimentally measured [12]. Thus our MD simulation results for the $T_g$ of pure PEO and PVC are consistent with experimental data. To the best of our knowledge, no experimental $T_g$ data are currently available for PEO/PVC blends.

To closely examine the energy contributions at $T_g$, Fig. 3 shows the energy per repeat unit as a function of temperature for the blends and pure systems. The bond stretching energy appears almost identical for all the five systems. The angle bending, dihedral torsion, non-bonded and Coulombic energies decrease with increasing PVC composition, while the van der Waal energy exhibits the opposite trend. With decreasing temperature, the bond stretching and angle bending energies decrease linearly and there is no discernible kink. The non-bonded energy does not show obvious kink; however, after decomposed into Coulombic and van

**Table 3**
Solubility parameters of pure PEO and PVC at different temperatures.

| $T$ (K) | $\delta_{PVC}$ | $\delta_{PEO}$ | $(\delta_{PVC} - \delta_{PEO})^2$ | $V_{mono}$[a] | $\chi$ from Eq. (5) |
|---|---|---|---|---|---|
| 480 | 16.13 ± 0.32 | 15.19 ± 0.69 | 0.88 | 46.38 | 0.010 |
| 460 | 16.38 ± 0.35 | 15.53 ± 0.46 | 0.72 | 45.86 | 0.0086 |
| 440 | 16.37 ± 0.37 | 15.93 ± 0.56 | 0.19 | 45.63 | 0.0024 |
| 420 | 16.66 ± 0.49 | 16.45 ± 0.51 | 0.04 | 44.89 | 0.0006 |
| 400 | 16.80 ± 0.55 | 16.95 ± 0.51 | 0.02 | 44.36 | 0.0003 |
| 380 | 16.93 ± 0.40 | 17.30 ± 0.54 | 0.13 | 43.67 | 0.0018 |
| 360 | 17.18 ± 0.51 | 17.88 ± 0.45 | 0.49 | 43.12 | 0.0071 |
| 340 | 17.35 ± 0.54 | 18.35 ± 0.34 | 1.00 | 42.65 | 0.015 |
| 320 | 17.47 ± 0.53 | 18.99 ± 0.34 | 2.32 | 42.18 | 0.037 |
| 300 | 17.61 ± 0.45 | 19.41 ± 0.46 | 3.22 | 41.80 | 0.054 |
| 280 | 17.72 ± 0.43 | 19.95 ± 0.25 | 4.94 | 41.49 | 0.088 |
| 260 | 17.86 ± 0.46 | 20.35 ± 0.41 | 6.21 | 40.92 | 0.12 |
| 240 | 17.98 ± 0.46 | 20.53 ± 0.45 | 6.52 | 40.67 | 0.13 |
| 220 | 18.10 ± 0.48 | 20.81 ± 0.43 | 7.39 | 40.33 | 0.16 |
| 200 | 18.13 ± 0.46 | 21.10 ± 0.39 | 8.82 | 40.05 | 0.21 |

[a] $V_{mono}$ was calculated from MD simulation for 50/50 PEO/PVC at 1 bar.

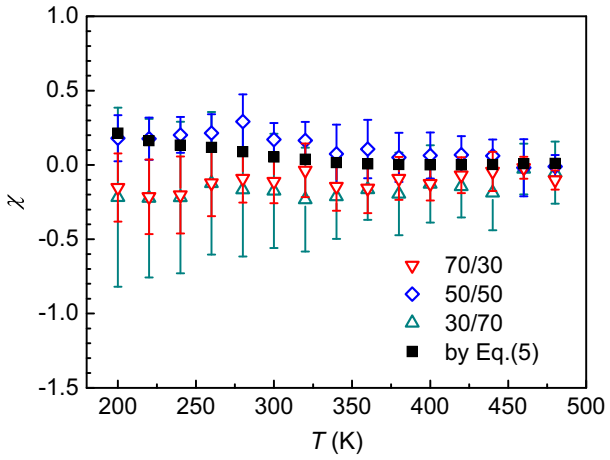


**Fig. 4.** Flory-Huggins parameter $\chi$ as a function of temperature from MD simulations for PEO/PVC blends with compositions of 70/30 (▽), 50/50 (◇), and 30/70 (△). For comparison, $\chi$ was also calculated by the solubility parameters (■).

der Waals energies, the kink is observed in the van der Waals energy. Despite the absence of kink, the Coulombic energy contributes largely to the non-bonded energy. Fig. 3 reveals that the torsion and van der Waals energies behave similarly to the specific volume in terms of temperature variation and play a dominant role in the glass transition. The occurrence of kink is due to the sudden "frozen" of the chains, which considerably decreases the degree of freedom in the torsion and van der Waals interactions; in contrast, the bond stretching and angle bending remain largely unperturbed.

### 3.2. Solubility and Flory–Huggins parameters

Solubility parameter is one of the important quantities for polymers and it characterizes the strength of attractive interactions. The solubility parameter $\delta$ is defined as:

$$\delta = \sqrt{\frac{E_{coh}}{V}} = \sqrt{\frac{E_{vac} - E_{bulk}}{V}} = \sqrt{CED} \tag{4}$$

where $E_{coh}$ is the cohesive energy per mole obtained from the energy difference between the molecule in vacuum ($E_{vac}$) and in amorphous bulk state ($E_{bulk}$). $V$ is the mole volume and $E_{coh}/V$ is the cohesive energy density also called CED. Empirically, if $(\delta_A - \delta_B)^2$ between two polymers A and B is less than 4 J/cm$^3$ [41,42], the two polymers would be expected miscible. This approach is only useful to judge the miscibility of simple systems in which the specific interactions (such as H-bonds) or non-combinatorial entropy effect (such as volume change induced by packing) do not play a dominate role. Flory–Huggins parameter $\chi$ could be estimated from

$$\chi = \frac{V_{mono}}{RT}(\delta_A - \delta_B)^2 \tag{5}$$

where $V_{mono}$ is a monomer unit volume per mole. $R$ is gas constant, and $T$ is temperature. For PEO/PVC blends, $V_{mono}$ was calculated by dividing the total volume of mixture by the number of repeat units in the system. Estimated from eq. (5), $\chi$ is always positive. As we shall discuss, this is not exactly correct.

If a binary blend is sufficiently equilibrated, the energy change of mixing could be calculated [43],

$$\Delta E_{mix} = \phi_A\left(\frac{E_{coh}}{V}\right)_A + \phi_B\left(\frac{E_{coh}}{V}\right)_B - \left(\frac{E_{coh}}{V}\right)_{mix} \tag{6}$$

where $\Delta E_{mix}$ is the energy change of mixing per unit volume, $\phi_A$ and $\phi_B$ are the volume fractions of polymer A and B, $\phi_A + \phi_B = 1$. The subscript "mix" denotes that the CED is for mixture. The Flory–Huggins parameter is thus evaluated by [43]:

$$\chi = \left(\frac{\Delta E_{mix}}{RT}\right)V_{mono} \tag{7}$$

Unlike Eq. (5), Eq. (7) gives either positive or negative $\chi$. A positive $\chi$ does not necessarily indicate that the blend is immiscible. Based on the Flory–Huggins theory, $\chi_c$ at the critical point is

$$x_c = 1/2\left(\frac{1}{\sqrt{n_A}} + \frac{1}{\sqrt{n_B}}\right)^2 \tag{8}$$

where $n_A$ and $n_B$ represent the number of repeat units of polymer A and B, respectively. If $\chi \le \chi_c$, the blend is considered to be miscible.

Table 3 lists the solubility and Flory–Huggins parameters as a function of temperature. With decreasing temperature, $(\delta_A - \delta_B)^2$ becomes larger and the calculated $\chi$ from Eq. (5) also increases, which implies that the blend is less miscible at a lower temperature. Eq. (5) only considers the difference in the CEDs between two polymers by assuming that the polymers with similar solubility parameters are mutual miscible. Alternatively, $\chi$ of blends can be evaluated by Eq. (7) assuming that realistic mixing or demixing systems are well generated. Fig. 4 shows $\chi$ as a function of temperature calculated by both Eq. (5) and Eq. (7). The large error bars were associated with the large fluctuations in the calculations of CEDs. It can be seen that PEO/PVC 50/50 blend has a positive $\chi$ in the whole temperature range and $\chi$ increases as temperature decreases, which is consistent with the result calculated by Eq. (5).

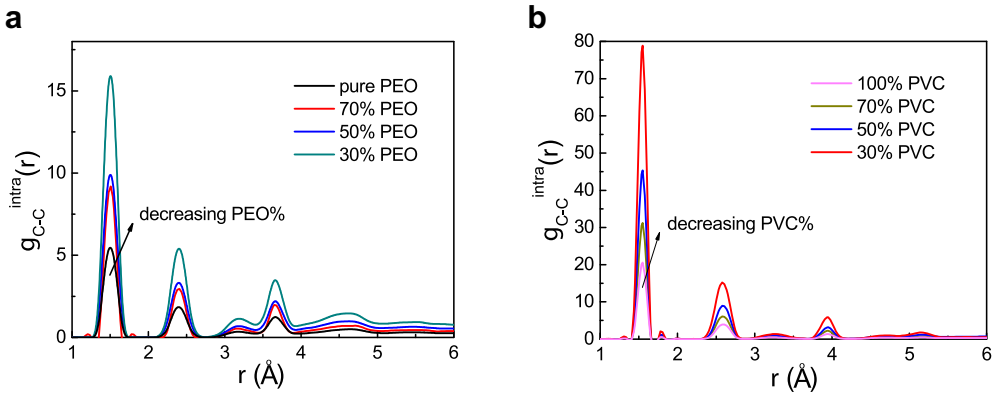


**Fig. 5.** Radial distribution functions of the intra-molecular carbon atoms of (a) PEO and (b) PVC at 300 K.

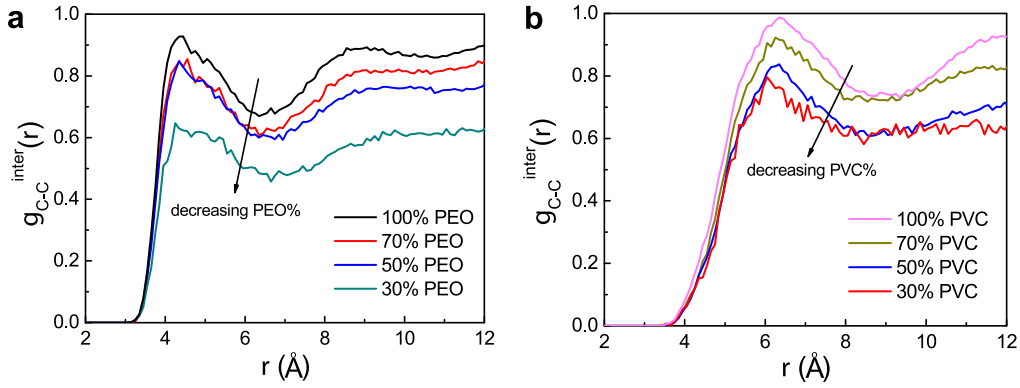


**Fig. 6.** Radial distribution functions of the inter-molecular carbon atoms of (a) PEO and (b) PVC at 300 K.

In contrast, PEO/PVC 30/70 and 70/30 blends have negative $\chi$, which changes marginally with temperature. Thus, our results are consistent with Etxeberria et al. [18], in which PEO/PVC 50/50 was found to be less compatible than the blend rich in PEO or PVC. The estimated $\chi$ values for the PEO/PVC 70/30 and 30/70 blends at 300 K are −0.12 and −0.17, respectively; consistent with experimental data ranging from −0.02 to −0.3 [14–16,19,44]. For PEO/PVC 50/50 blend, $\chi$ is approximately 0.17 evaluated from MD simulation and higher than measured result −0.02 [14,18]. The deviation between simulation and experimental $\chi$ could attribute primarily to two reasons. First, the polymers used in simulations were relatively shorted compared to real samples. Second, the force field used may not be able to capture all the detailed interactions.

### 3.3. Radial distribution functions and hydrogen bonds

Radial distribution function $g(r)$ is commonly used to characterize molecular structure. This function represents the probability of finding a pair of atoms at a distance $r$ with respect to the bulk phase in a completely random distribution. It is defined as,

$$g_{AB}(r) = \frac{1}{\rho_{AB} 4\pi r^2} \frac{\sum_{t=1}^{K} \sum_{j=1}^{N_{AB}} \Delta N_{AB}(r \to r + \delta r)}{N_{AB} \times K} \quad (9)$$

where $N_{AB}$ is the total number of atoms of A and B in the system, $K$ the number of time steps, $\delta r$ the distance interval, $\Delta N_{AB}$ the number of B (or A) atoms between $r$ to $r + \delta r$ around an A (or B) atom, $\rho_{AB}$ the bulk density. Note that A and B could be the same type of atoms. It has been observed that if a binary system is compatible, the inter-molecular $g(r)$ of AB pair between two different polymers are larger than those of AA and BB pairs [45].

Fig. 5 shows $g(r)$ of the intra-molecular carbon atoms of PEO and PVC in the pure and blend systems. For PEO chain, the highest peak is at 1.5 Å, which simply indicates bond connectivity. The atomic pairs without connectivity have the spatial vicinities at 2.4 Å for the first adjacent pairs and at 3.7 Å for the second adjacent pairs. As the PEO composition decreases from 100% to 30%, the peaks become higher which is caused primarily by the decrease of PEO bulk density in the denominator of Eq. (9). For PVC chain, the peaks illustrating bond connectivity, the first adjacent and the second adjacent atomic pairs are located at 1.5, 2.6 and 3.9 Å, respectively. Similar to PEO, the peak values also increase with increasing PVC composition.

The $g(r)$ of the inter-molecular atomic pairs could indicate the interactions of polymer chains. Fig. 6 shows the $g(r)$ of the inter-molecular carbon atoms of PEO or PVC chains themselves in pure and blend systems. For pure PEO, there is a distinct peak at 4.4 Å and the second peak is located at 8.6 Å. The value of $g(r)$ decreases with decreasing PEO composition, which implies that the adjacent interactions between different PEO chains become weaker upon adding PVC. The change tendency of $g(r)$ for PVC chains is very similar. The first peak is located around 6.3 Å and the value decreases as decreasing PVC composition. The second peak appears beyond 12 Å for PVC, but not obvious because of relatively small simulation box used.

We also calculated the $g(r)$ of the inter-molecular carbon atomic pairs of PEO-PVC, PEO–PEO and PVC–PVC chains in the three blends. As shown in Fig. 7, the $g(r)$ of PEO-PVC is higher than those of PEO–PEO and PVC–PVC in all the three blends, particularly in PEO/PVC 70/30 and 30/70 blends. More interestingly, the first peak in the $g(r)$ of PEO-PVC for 50/50 blend is about 0.95 and smaller than those of another two blends (about 1.1). This confirms that the $g(r)$ of the unlike-component is usually higher than that of like-component in a miscible system [45–47]. Thus, the $g(r)$ of the inter-molecular carbon atomic pairs also indicates that PEO/PVC blends are more miscible when they are rich in PEO or PVC.

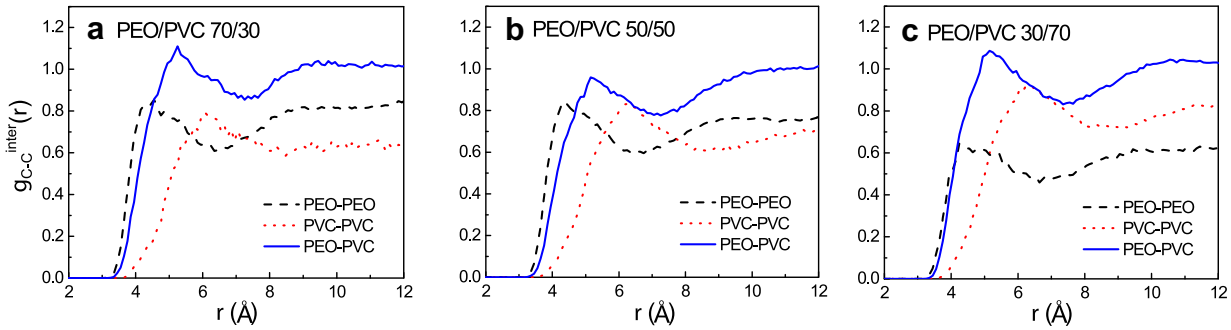


**Fig. 7.** Radial distribution functions of the inter-molecular carbon–carbon pairs of like and unlike components in PEO/PVC blends.

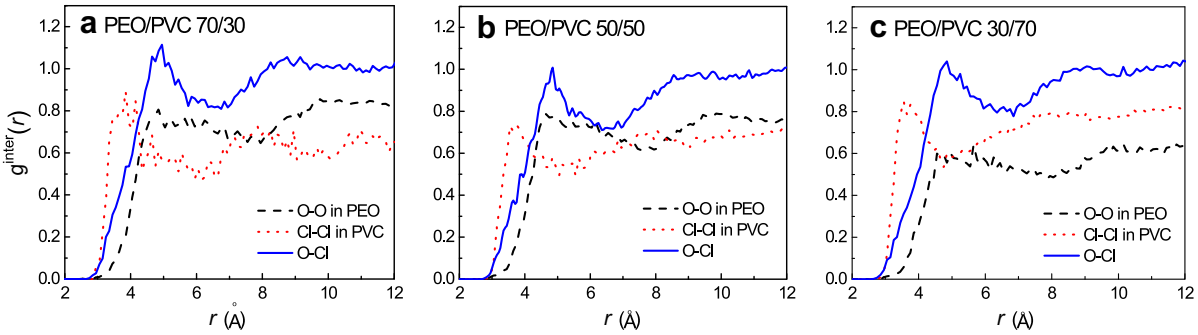


**Fig. 8.** Radial distribution functions between O atoms in PEO, Cl atoms in PVC, and O–Cl pairs in PEO and PVC.

Fig. 8 further shows the $g(r)$ between O atoms in PEO and the Cl atoms in PVC, as well as the O–O pairs of PEO and the Cl–Cl pairs of PVC. The O–Cl pairs have a higher $g(r)$ than those of O–O and Cl–Cl pairs in all the three blends. This is attributed to the factor that O is electro-rich in PEO chains, while Cl in PVC chains is electro-deficient; therefore, they form attractive electrostatic interactions [14,19,20]. This indicates the preferential O–Cl interactions in the blends over the O–O and Cl–Cl interactions. In addition, the $g(r)$ of O–Cl pairs in PEO/PVC 30/70 and 70/30 blends has larger values than in 50/50 blend. Again, this confirms that 30/70 and 70/30 blends are more miscible than 50/50 blend.

Hydrogen bonds between the donor C atoms (CHCl groups) of PVC and the acceptor O atoms in PEO were also examined. The formation of H-bond should satisfy three criteria in this study: first, the distance between proton and acceptor is less than a specific cutoff; second, the angle among donor C, H proton and acceptor O is greater than 90°; third, acceptor O only receives one proton and an H proton only forms an H-bond with one O. Table 4 lists the percentage of H-bond at two different cutoff ($r_{cut}$) 2.5 and 3.0 Å, respectively. The percentage was calculated in terms of the number of formed H-bonds divided by total number of O atoms (for proton-rich system) or H atoms (for acceptor-rich system). PEO and PVC indeed form weak H-bonds with a percentage larger than 2.2% within $r_{cut} \leq 2.5$ Å, while the percentage increases to over 9.9% at $r_{cut} = 3.0$ Å. The probability of H-bonding is higher in PEO/PVC 70/30 and 30/70 blends compared to that in 50/50 blend. Consistent with the above findings, this reveals that 70/30 and 30/70 blends are more miscible.

### 3.4. Dynamics of polymer chains

Recently, Lodge and McLeish proposed a novel method to describe the local dynamics in a miscible polymer blend [48]. The method accounts for the self-concentration effect, that is, the local composition of a monomer is always higher than the macroscopic composition as a direct consequence of chain connectivity. Therefore, the local segmental dynamics (relaxation time) of polymer chains in a blend would exhibit different temperature and composition dependences. This method has been successfully used to analyze the segmental dynamics in polymer mixtures [49,50].

**Table 4**
Percentage of H-bond between O atoms in PEO and H atoms of CHCl group in PVC. $r_{cut}$ is the cutoff distance between O and H atoms.

| PEO/PVC ratio | $r_{cut} = 2.5$ Å | $r_{cut} = 3.0$ Å |
|---|---|---|
| 70/30 | 3.45 ± 1.58% | 15.57 ± 3.62% |
| 50/50 | 2.20 ± 0.53% | 9.90 ± 1.86% |
| 30/70 | 2.54 ± 0.74% | 11.59 ± 2.75% |

In order to investigate the dynamics of PEO and PVC chains in our study, the mean-squared displacements (MSD) were estimated from the last 100-ps trajectory in MD simulations,

$$\mathrm{MSD} = \left\langle |r(t) - r(0)|^2 \right\rangle \tag{10}$$

where $r(t)$ and $r(0)$ are the positions of the centre of mass of molecules at time $t$ and 0, respectively. Fig. 9 shows the MSDs of PEO and PVC in pure PEO and PVC as well as their blends. Compared to pure PEO, the addition of PVC decreases the mobility of PEO chains in all the three blends. In contrast, the mobility of PVC chains increases as its composition decreases from 100% to 30%. The results are consistent with the crystallization experiment of PEO/

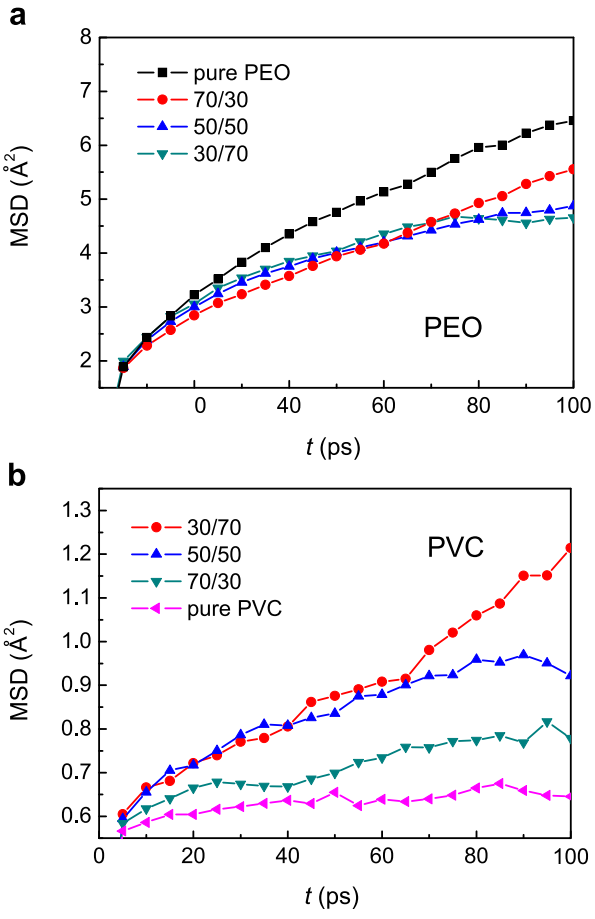


**Fig. 9.** Mean-squared displacements of (a) PEO and (b) PVC in pure PEO and PVC and their blends.

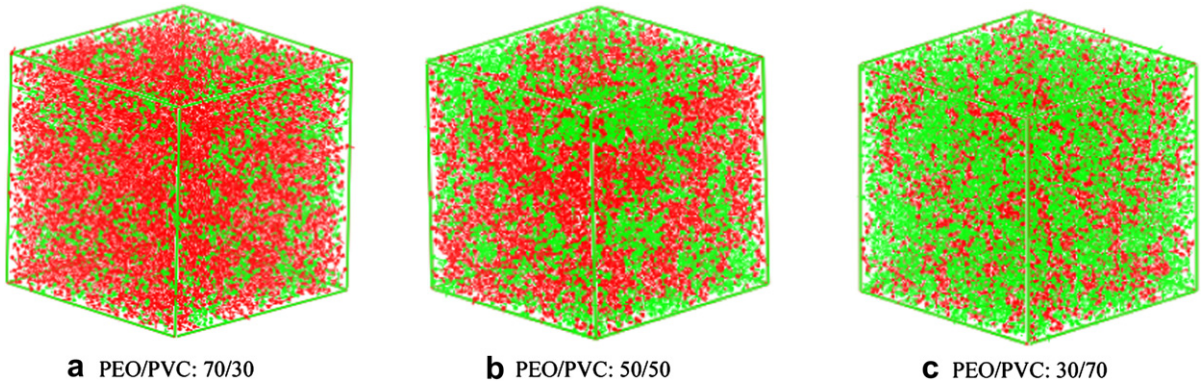


**Fig. 10.** Morphologies of PEO/PVC blends from DPD simulations. PEO: red, PVC: green.

PVC, which indicates that adding PVC into PEO would decrease the relaxation rate of PEO chains, thus suppresses PEO crystallization rate as well as crystallization temperature [14–16]. Our simulations also imply that the enhanced mobility of PVC is due to the decrease in the crystallization rate of PEO.

### 3.5. Morphologies

From the fully atomistic MD simulations, $\chi$ values at 300 K are estimated to be −0.12, 0.17, −0.17 for PEO/PVC 70/30, 50/50 and 30/70 blends, respectively. The $\chi$ value for 50/50 blend is larger than the critical value $\chi_c = \frac{1}{2}(1/\sqrt{142} + 1/\sqrt{100})^2 = 0.017$. Therefore, as discussed earlier, phase separation might occur in 50/50 blend. To further explore the possible phase transition in the three blends, DPD simulations were performed with $a_{AB}$ values listed in Table 2. Fig. 10 illustrates the morphologies of the three blends after $2 \times 10^5$ time steps. By visualization, PEO and PVC mix fairly well in 70/30 and 30/70 blends, whereas PEO and PVC-rich domains are observed in 50/50 blend. This demonstrates the weak phase separation occurs in the 50/50 blend.

## 4. Conclusions

Fully atomistic MD and mesoscale DPD simulations have been adopted to investigate the miscibility of PEO/PVC blends. It is found that 40 repeat units are sufficient to represent a PEO chain and 50 for a PVC chain. Based on the temperature dependence of specific volume, a single glass transition occurs in three blends at compositions of 70/30, 50/50 and 30/70, which indicates PEO and PVC are miscible. The glass transition temperature increases with increasing PVC composition. The angle bending, dihedral torsion, and Coulombic energies decrease with increasing PVC composition, while the reverse is true for van der Waal energy. The dihedral torsion and van der Waals energies exhibit similar behavior to the specific volume and play an important role in the glass transition of PEO/PVC blends. The Flory-Huggins parameter $\chi$ for PEO/PVC 50/50 blend is positive in the whole temperature range and increases with decreasing temperature. Nevertheless, $\chi$ for PEO/PVC 30/70 and 70/30 is negative and varies slightly with temperature. Our simulations reveal that PEO/PVC 50/50 blend is less miscible than 70/30 and 30/70 blends. The radial distribution functions of the inter-molecular carbon atoms also indicate that 50/50 blend is less miscible. The specific electrostatic attractions between O and Cl atoms, as well as the H-bonds between O atoms of PEO and H atoms of PVC, contribute to the miscibility of PEO and PVC. The morphologies obtained by DPD simulations further demonstrate that 50/50 blend is less miscible than 70/30 and 30/70 blends and exhibits a weak phase separation. The dynamics of PEO chains decreases upon the addition of PVC, which is consistent with the experimental observation that the crystallization rate of PEO decreases in PEO/PVC blends compared to pure PEO.

## Acknowledgement

The authors are grateful for the financial supports from the Singapore National Research Foundation on the Competitive Research Programme (R-279-000–261–281).

## References

[1] Lin H, Freeman BD. Journal of Membrane Science 2004;239:105.
[2] Lin HQ, Freeman BD. Journal of Molecular Structure 2005;739:57.
[3] Alangari AA, Kennerley JW, Newton JM. Journal of Pharmacy and Pharmacology 1985;37:151.
[4] Al-Nasassrah MA, Podczeck F, Newton JM. European Journal of Pharmaceutics and Biopharmaceutics 1998;46:31.
[5] Hirayama Y, Kase Y, Tanihara N, Sumiyama Y, Kusuki Y, Haraya K. Journal of Membrane Science 1999;160:87.
[6] Lin HQ, Van Wagner E, Swinnea JS, Freeman BD, Pas SJ, Hill AJ, et al. Journal of Membrane Science 2006;276:145.
[7] Bondar VI, Freeman BD, Pinnau I. Journal of Polymer Science, Part B: Polymer Physics 1999;37:2463.
[8] Bondar VI, Freeman BD, Pinnau I. Journal of Polymer Science, Part B: Polymer Physics 2000;38:2051.
[9] Kawakami M, Iwanaga H, Hara Y, Iwamoto M, Kagawa S. Journal of Applied Polymer Science 1982;27:2387.
[10] Li JT, Wang SC, Nagai K, Nakagawa T, Mau AWH. Journal of Membrane Science 1998;138:143.
[11] Li JT, Nagai K, Nakagawa T, Wang S. Journal of Applied Polymer Science 1995;58:1455.
[12] Brandrup J, Immergut EH, Grulke EA, Abe A, Bloch D. Polymer handbook. 4th ed. Wiley-Interscience; 1999.
[13] Ramesh S, Winie T, Arof AK. European Polymer Journal 2007;43:1963.
[14] Castro REN, Toledo EA, Rubira AF, Muniz EC. Journal of Materials Science 2003;38:699.
[15] Marco C, Gómez MA, Fatou JG, Etxeberria A, Elorza MM, Iruin JJ. European Polymer Journal 1993;29:1477.
[16] Katime IA, Anasagasti MS, Peleteiro MC, Valenciano R. European Polymer Journal 1987;23:907.
[17] Sadeghi M, Chenar MP, Rahimian M, Moradi S, Dehaghani AHS. Journal of Applied Polymer Science 2008;110:1093.
[18] Etxeberria A, Elorza JM, Iruin JJ, Marco C, Gómez MA, Fatou JG. European Polymer Journal 1993;29:1483.
[19] Neiro SMD, Dragunski DC, Rubira AF, Muniz EC. European Polymer Journal 2000;36:583.
[20] Ramesh S, Yahaya AH, Arof AK. Solid State Ionics 2002;148:483.
[21] Margaritis AG, Kalfoglou NK. Journal of Polymer Science, Part B: Polymer Physics 1988;26:1595.
[22] Materials studio 4.3. San Diego: Accelrys; 2008.
[23] Theodorou DN, Suter UW. Macromolecules 1985;18:1467.
[24] Theodorou DN, Suter UW. Macromolecules 1986;19:139.
[25] Meirovitch H. Journal of Chemical Physics 1983;79:502.
[26] Sun H. Journal of Physical Chemistry B 1998;102:7338.
[27] Rigby D, Sun H, Eichinger BE. Polymer International 1997;44:311.
[28] Sun H, Ren P, Fried JR. Computational and Theoretical Polymer Science 1998;8:229.

[29] Berendsen HJC, Postma JPM, van Gunsteren WF, Dinola A, Haak JR. Journal of Chemical Physics 1984;81:3684.
[30] Bicerano J. Prediction of polymer properties. 3rd ed. New York: Marcel Dekker Inc; 2002.
[31] Hoogerbrugge PJ, Koelman JMVA. Europhysics Letters 1992;19:155.
[32] Groot RD, Warren PB. Journal of Chemical Physics 1997;107:4423.
[33] Spyriouni T, Vergelati C. Macromolecules 2001;34:5306.
[34] Jawalkar SS, Adoor SG, Sairam M, Nadagouda MN, Aminabhavi TM. Journal of Physical Chemistry B 2005;109:15611.
[35] Ahmadi A, Freire JJ. Polymer 2009;50:4973.
[36] Jawalkar SS, Aminabhavi TM. Polymer 2006;47:8061.
[37] Yang H, Li ZS, Qian HJ, Yang YB, Zhang XB, Sun CC. Polymer 2004;45:453.
[38] Yang H, Li ZS, Lu ZY, Sun CC. European Polymer Journal 2005;41:2956.
[39] Mark JE. Polymer data handbook. 3rd ed. USA: Oxford University Press; 1999.
[40] Faucher JA, Koleske JV, Santee Jr ER, Stratta JJ, Wilson III CW. Journal of Applied Physics 1966;37:3962.
[41] Abou-Rachid H, Lussier LS, Ringuette S, Lafleur-Lambert X, Jaidann M, Brisson J. Propellants Explosives Pyrotechnics 2008;33:301.
[42] Mason JA, Sperling LH. Polymer blends and composites. New York: Plenum Press; 1976.
[43] Case FH, Honeycutt JD. Trends in Polymer Science 1994;2:259.
[44] Huang XD, Goh SH. Polymer 2002;43:1417.
[45] Akten ED, Mattice WL. Macromolecules 2001;34:3389.
[46] Gestoso P, Brisson J. Polymer 2003;44:2321.
[47] Suknuntha K, Tantishaiyakul V, Vao-Soongnern V, Espidel Y, Cosgrove T. Journal of Polymer Science, Part B: Polymer Physics 2008;46:1258.
[48] Lodge TP, McLeish TCB. Macromolecules 2000;33:5278.
[49] He YY, Lutz TR, Ediger MD. Journal of Chemical Physics 2003;119:9956.
[50] May AF, Maranas JK. Journal of Chemical Physics 2006;125:024906.